



Nanostructured lipid carriers loaded with Halobetasol propionate for topical treatment of inflammation: Development, characterization, biopharmaceutical behavior and therapeutic efficacy of gel dosage forms

Paulina Carvajal-Vidal^{a,b}, Roberto González-Pizarro^{a,b,d,2}, Carolina Araya^{a,e,3}, Marta Espina^{a,b}, Lyda Halbaut^a, Immaculada Gómez de Aranda^c, M. Luisa García^{a,b,*}, Ana C. Calpena^{a,b,1}

^a Pharmacy, Pharmaceutical Technology and Physical Chemistry Department, Faculty of Pharmacy and Food Sciences, University of Barcelona, Av. de Joan XXIII, 27-31, 08028 Barcelona, Spain

^b Institute of Nanoscience and Nanotechnology (IN2UB), University of Barcelona, 08028 Barcelona, Spain

^c Pathology and Experimental Therapeutics Department, Faculty of Medicine and Health Sciences, Bellvitge Campus, University of Barcelona, Av. Mare de Déu de Bellvitge, 3, 08907 L'Hospitalet de Llobregat, Barcelona, Spain

^d National Drug Agency Department (ANAMED), Institute of Public Health (ISP), Av. Marathon 1000, Ñuñoa, 7780050 Santiago, Chile

^e Bussiness Manufacturing Company of Ecuador, Av Republica E3-33, 170103 Quito, Ecuador

ARTICLE INFO

Keywords:

Halobetasol propionate
NLC
Stability improvements
Rheological assessment
Skin inflammation
Drug delivery
Skin permeation

ABSTRACT

The aim of this research was the development and characterization of three gel dosage forms of Halobetasol propionate loaded lipid nanoparticles (HB-NLC) for the treatment of inflammatory skin diseases. A Pluronic gel (PI-HB-NLC), a Carbopol gel (Cb-HB-NLC) and a Cremigel (Cg-HB-NLC), were characterized for stability, swelling, degradation, porosity and rheology. The biopharmaceutical behavior of *in vitro* release and *ex vivo* permeation, along with microbiological stability were also evaluated. Tolerance and therapeutic efficacy were determined *in vivo*. The gels proved to have eudermic pH and to be effective to improve HB-NLC stability for more than 6 months. *In vitro* drug release profiles were adjusted to a first order (PI-HB-NLC, Cg-HB-NLC) and hyperbola (Cb-HB-NLC) kinetic models, revealing sustained drug release. *Ex vivo* biopharmaceutical behavior showed slow drug penetration through skin, delaying the drug entrance into systemic circulation. The formulations were effective in reducing inflammation with a lower drug dose in comparison with existing treatments, obtaining the fastest effect when using PI-HB-NLC. After application of the formulations in volunteers, no irritation, redness or edema reactions were detected, plus, an enhancement of the biomechanical properties of the skin was evidenced. Therefore, the results indicate that these formulations are a suitable alternative to current treatments.

1. Introduction

The skin is the largest organ in the body and its principal function is to separate the external from the internal environment. In the face of external (and sometimes internal) stimuli or aggressions, the skin responds in a non-specific and innate way, triggering the inflammatory process (Pasparakis et al., 2014). This process is generally characterized by the presence of edema, increased temperature, itching and redness of the area. Diseases such as psoriasis, allergies, atopic dermatitis and

eczema usually produce this type of symptomatology chronically (Boguniewicz and Leung, 2011; Eyerich and Novak, 2013). Due to their great anti-inflammatory action, corticosteroid are drugs of choice for a wide variety of skin diseases (Al-Dabagh et al., 2014). They have several mechanisms of action which allow them to produce local and systemic effects (Ramamoorthy and Cidlowski, 2016). Derived from its multiple mechanisms of action, together with the desired treatment, undesirable local effects such as pigmentation and skin thinning or systemic effects such as metabolic alterations like Cushing's syndrome

* Corresponding author at: Pharmacy, Pharmaceutical Technology and Physical Chemistry Department, Faculty of Pharmacy and Food Sciences, University of Barcelona, Av. de Joan XXIII, 27-31, 08028 Barcelona, Spain.

E-mail addresses: marisagarcia@ub.edu, rdrm@ub.edu (M.L. García).

¹ Co-author: Ana Calpena.

² Present address: National Drug Agency Department (ANAMED), Institute of Public Health (ISP), Av. Marathon 1000, Ñuñoa, 7780050 Santiago, Chile.

³ Present address: Bussiness Manufacturing Company of Ecuador, Av Republica E3-33, 170103 Quito, Ecuador.

can be produced (Dhar et al., 2014). To improve their characteristics, whether controlling their potency, increasing their desired effects or reducing side effects, different semisolid dosage forms for topical administration have been developed. Creams, gels and lotions have been used for the treatment of diverse skin diseases (Herz et al., 1991; Mancuso et al., 2003; Lowe et al., 2005). Along with this, there are other more technological methods of dosage forms such as the first and second generation of lipid nanoparticles, known as solid lipid nanoparticles (SLN) and nanostructured lipid carrier (NLC), respectively (Müller et al., 2000, 2007). Lipid nanoparticles have been extensively studied to control the penetration and effects of corticosteroids generally considered “high potency”, because they are the most likely to cause severe adverse effects, reason why, traditional treatments are recommended for short periods of time (two weeks) despite many times, treating diseases with chronic symptoms (Coureau et al., 2008; Jensen et al., 2010; Bikkad et al., 2014; Carvajal-Vidal et al., 2019).

With the aim to allow prolonged treatments reducing potential systemic side effects, improve skin characteristics and promote the local effect of a “super potent” corticosteroid, over its systemic action, three topical gel dosage forms based on Pluronic (Pl-HB-NLC), Carbopol (Cb-HB-NLC) and Sepigel® (Cg-HB-NLC), containing Halobetasol propionate (HB) loaded nanostructured lipid carriers (NLC), with a 20% of the regular dose have been developed to obtain a new controlled release system of HB as an alternative to current topical treatments.

2. Materials and methods

2.1. Materials

HB was obtained from Capot Chemical Company Limited (Hangzhou, China), LAS (PEG-8 caprylic/capric glycerides) and Precirol ATO® 5 (Glyceryl distearate) were kindly gifted from Gattefossé (Madrid, Spain). Tween® 80 (Polysorbate 80), Isopropyl myristate and Glycerin, were purchased to Sigma Aldrich (Madrid, Spain). Sepigel® 305 (Sep) was bought from Seppic (Paris, France). Polymers Carbopol® 940 (Cb) and Pluronic® F-127 (Pl) were obtained from Fagron Iberica (Terrassa, Spain). All others chemical reagents and components used in this research were of analytical grade. A Millipore Milli-Q Plus system was used to obtain purified water.

2.2. Gel elaboration

HB-NLC suspension was previously produced by high-pressure homogenization method (Homogeniser FPG 12800, Stansted, United Kingdom) (Neupane et al., 2014) with Tween® 80 as surfactant and LAS and Precirol ATO 5® as liquid lipid and solid lipid respectively, as described elsewhere (Carvajal-Vidal et al., 2019).

Three gels were prepared at room temperature with the HB-NLC suspension used instead of pure water. Cg-HB-NLC was prepared by driving the aqueous phase (HB-NLC and glycerin 10%) over the oil phase (Sep 3%, isopropyl myristate 3%) under constant magnetic agitation until mixture homogenization. Cb-HB-NLC was made with 2% (w/v) of polymer and 1% (w/v) of glycerin dissolved directly in HB-NLC suspension under magnetic stirring for 24 h. After, the formulation was stabilized with triethanolamine to ensure a eudermic pH. Pl-HB-NLC was made gradually dissolving the polymer (20%) into the HB-NLC suspension under continuous agitation until there was no residual powder. All formulations after preparation were stored at 4 and 25 °C until following studies.

2.3. Macroscopic and microscopic determinations

The gels were macroscopically studied for color, viscosity and odor immediately and six months after being prepared, to detect visual changes or any instability signs such as phase separation, precipitation or creaming. Fresh formulations were microscopically analyzed to

evaluate their droplet size and homogeneity degree using an optical Leica DM 1000 LED light microscope (Leica Microsystems, Wetzlar, Germany) with a camera Leica EC3 (Leica Microsystems, Wetzlar, Germany) at 40x magnifying power, images were taken directly from the formulations without dilution. Meanwhile, the pH was measured with a CRISON micro-pH 200 microprocessor controlled pH-meter (Crison Instruments S.A., Barcelona, Spain) at room temperature (25 °C).

Additionally, the structure of the formulations was studied by Scanning Electron Microscopy (SEM) with a J-7001F (JEOL Inc., MA, USA) with a secondary electron detector (Everhart-Thornley type). The sample was deposited directly on the microscope sample holder, and the subsequent observation was carried out, without the need to coat them, under high vacuum and low voltage (1 kV) conditions (Barshack et al., 2004).

2.4. Rheological behavior and extensibility

Rheological measurements were determined for each formulation using a rotational Haake RheoStress RS1 rheometer (Thermo Fisher Scientific, Karlsruhe, Germany) prepared with a cone-plate geometry (Haake C60-2° Ti, 60 mm diameter, 0.106 mm gap between plates) connected to a temperature control device at 25 °C (Thermo Haake Phoenix II + Haake C25P). The data were recorded with samples under a program consisting of 3 steps. First, a period of ramp-up from 0 to 50 s⁻¹ for 3 min. Second, a constant shear rate period at 50 s⁻¹ during 1 min. Third, a ramp-down period from 50 s⁻¹ to 0 during 3 min. From the constant shear stretch at 50 s⁻¹, the steady-state viscosity was also determined. Pl-HB-NLC sol-gel transition temperature was determined placing the gel in a water bath under continuous stirring with a magnetic bar. The temperature of the gel was gradually increased from 20 to 38 °C. It was considered that the gelation temperature was reached when the magnetic bar stopped (Brugués et al., 2015). The experiment was accomplished by triplicate.

The extensibility index was determined at room temperature by setting 25 mg of gel between two millimeter microscope slides. The samples were compressed by placing increasing weights (2, 5, 10, 20, 50 and 100 g) on it for 30 s. The diameter (mm) of the formed circle by the gel was noted. For each weight, a diameter of gel was obtained with which the increase in surface area (mm²) of the formulation was calculated as a function of the increasing weights applied (Campañá-Seoane et al., 2014). The experiment was accomplished by triplicate.

2.5. Swelling, degradation and porosity index

The swelling ratio (SR), the degradation tests and the porosity index (P) were evaluated by a gravimetric method. To evaluate the SR of each formulation, a specified weight of dried gels were immersed in PBS solution (pH = 5.5 at 32 °C) for 1.5 h. for Cb-HB-NLC, 24 min. for Cg-HB-NLC and 4 min. for Pl-HB-NLC. At defined times, previously determined, the samples were taken out from the solution and the weight gain due to PBS uptake was measured. The test was performed in triplicate and the SR% was calculated based on the following equation:

$$SR\% = \frac{(W_s - W_d)}{W_d} \cdot 100 \quad (1)$$

where W_s represent the weight of swollen gel at different times and W_d is the initial dried gel weight (Zhao et al., 2005; Lee and Bucknall, 2008).

Degradation test was calculated as percentage of weight loss (WL) by immersing weighted amounts of fresh gel in a PBS solution (pH = 5.5 at 32 °C) during 6.5 h. for Cb-HB-NLC, 1 h. for Cg-HB-NLC and 80 min. for Pl-HB-NLC. At regular time intervals, the samples were withdrawal, the excess of water was removed and the weight was measured. WL was calculated using the equation:

$$WL(\%) = \frac{(W_i - W_d)}{W_i} \cdot 100 \quad (2)$$

where, W_i is the initial fresh gel weight and W_d is the gel weight at different time intervals (Mallandrich et al., 2017).

The P was measured by solvent replaced method. A total of 0.5 g of the dried gel was submerged in absolute ethanol. During different periods of time, the sample was weighted until constant weight. P was calculated based on the following equation:

$$P = \left(\frac{W_2 - W_1}{\rho \times V} \right) \cdot 100 \quad (3)$$

where, W_1 is the weight of the dried gel. W_2 is the final weigh of the gel (with ethanol), ρ is the density of absolute ethanol and V is the volume of applied gel to the test.

2.6. Stability test

Cg-HB-NLC, Cb-HB-NLC and Pl-HB-NLC were stored at 4 and 25 °C for 6 months. During this time, the physical stability of the formulations needed to be assessed. For this purpose, stability studies were carried out through the analysis of light backscattering (BS) by using a Turbiscan®Lab equipment to identify possible destabilization phenomena such as sedimentation or creaming (among others). A sample of 10 g of each gel was placed in a glass measuring cell. The radiation source used was a pulsed near infrared light-emitting diode LED ($\lambda = 880$ nm) read by a backscattering detector located at an angle of 45° from the incident beam. Measurements (one scan every five minutes during 15 min) were taken 1 day after preparation of the formulation and at 1, 2 and 6 months.

2.7. Microbiological stability

6 months after being prepared, the microbiological load in the gels was measured. The counting of viable mesophilic microorganisms was carried out through inoculation by inclusion in plates of TSA (Tryptona Soy Agar, OXOID Ref. CM131B) and Sabouraud Dextrose Agar supplemented with chloramphenicol (OXOID Ref. CM CM0041) for fungi and yeasts. The sample was incubated at 30 ± 2 °C for 5 days. To verify the absence of *E. coli*, *Staphylococcus aureus* and *Candida albicans*, 1 mL of each sample was inoculated in TSB broth tubes (Tryptona Soy Caldo de OXOID, Ref. CM0129B) and incubated at 35 ± 2 °C for 72 h. After that, striae by exhaustion were made in selective media for the microorganisms previously described (Ratajczak et al. 2015).

2.8. Biopharmaceutical behavior

2.8.1. In vitro release

To determine and compare the *in vitro* HB release of each gel, a study was carried out in Franz-type diffusion cells (FDC 400, Crown Glass, Somerville, NY, USA) (Gonzalez-Pizarro et al., 2019). A cellulose dialysis membrane, MW 12000–14000 Da (Iberoamerica, Spain) was selected and after hydration was placed between the donor and the receptor compartment with a diffusion area of 2.54 cm². For hydrating the membrane and as a receptor medium a solution of Transcutol®/water (70:30) was used. When starting the experiment, in the donor compartment, 300 mg of each gel were added in complete contact with the dialysis membrane. At determined times, samples of 300 μ l were collected from the receptor compartment with a syringe and replaced with new receptor medium. The test was carried out during 335 h. assuring sink conditions and a constant temperature of 32 ± 0.5 °C. The HB content in the samples was analyzed by RP-HPLC by a methodology described elsewhere (Carvajal-Vidal et al., 2017). The release test was performed by triplicate and the cumulative amount of HB, Akaike's information criterion (AIC) and correlation coefficient (r^2) were calculated to determine the best fitting release model (Ramos

et al., 2016) and to compare release characteristics between formulations.

Kinetic equations used to fit the amount of HB released:

$$\text{Zero order: } \frac{Q_t}{Q_\infty}(\%) = k \cdot t \quad (4)$$

$$\text{First order: } \frac{Q_t}{Q_\infty}(\%) = 1 - e^{-kt} \quad (5)$$

$$\text{Hyperbola: } \frac{dQ}{dt} = \frac{Vm \cdot Q}{Km + Q} \quad (6)$$

$$\text{Higuchi: } \frac{Q_t}{Q_\infty}(\%) = kh \cdot t^{1/2} \quad (7)$$

$$\text{Korsmeyer - Peppas: } \frac{Q_t}{Q_\infty}(\%) = k \cdot t^n \quad (8)$$

where Q_t corresponds to the amount of drug released at time (t), Q_∞ corresponds to the maximum amount of drug released, "k" is the release rate constant (concentration/t), and "n" is the diffusion release indicative of the drug release mechanism. (Costa & Sousa Lobo, 2001). V_m represents the maximum process speed and K_m corresponds to the amount of drug relative to a speed that is half of the maximum speed (Berrozpe et al., 2008).

2.8.2. Ex vivo skin permeation

For each formulation, a permeation test with human skin was performed in Franz-type cells (FDC 400, Crown Glass, Somerville, NY, USA) (Gonzalez-Pizarro et al., 2019) for a period of 36 h. The human skin was voluntary donated under informed consent by a female patient undergoing an abdominal plastic surgery. The procedure and the experimental protocol were approved by the Bioethics Committee of the Barcelona-SCIAS Hospital (Barcelona, Spain). Once obtained, the skin was frozen at -20 °C to facilitate its manipulation. Subsequently, based on international guidelines (Organization for Economic Co-Operation and Development; European Centre for the Validation of Alternative Methods), 0.4 mm thick pieces of skin cut with a dermatome (Model GA 630, Aesculap, Tuttlingen, Germany) were used as a permeation membrane. The skin was placed in the Franz cells between the donor compartment and the receptor compartment, with the stratum corneum facing the upper chamber and with a diffusion area of 0.64 cm². Once assembled, the skin barrier integrity was evaluated by measuring transepidermal water loss (TEWL) (TEWL-meter TM210, Courage & Khazaka, Koln, Germany) with the probe placed in the donor compartment very close to the skin. Human skin pieces exhibiting TEWL values below 10 g/(m²·h) were used for the experiment (Mallandrich et al., 2017). The temperature of the system was kept constant at 32 ± 2 °C by a thermoregulated water bath during the complete experiment, and a solution of Transcutol/water (70:30) was used as a receptor medium in the receptor compartment. A total of 300 mg of each formulation were placed on the donor compartment in direct contact with the skin membrane. At certain times, an aliquot of 300 μ l from the receptor chamber was withdrawn and replaced with fresh medium solution until 36 h. of contact. The quantity of permeated HB was determined by RP-HPLC. Later, permeation parameters such as flux (J), permeability coefficient (Kp), permeated amount at 36 h (A_{36}), were calculated using a linear least-squares regression model. The samples were performed by triplicate and evaluated in skin from the same donor to avoid variations in the response due to biological differences of the skin, and only detect differences due to characteristics of each formulation.

2.9. In vivo and ex vivo assays

2.9.1. Animals

Following the existing international guidelines (Organization for

Economic Co-Operation and Development (OECD, 2019), New Zealand male albino rabbits of 2.0–2.2 kg weight were used for the *in vivo* experimentation. Rabbits were kept in standard cages with food and water *ad libitum* and under controlled ambient conditions (25 ± 1 °C, 50–60% relative humidity). According with the Catalonian government regulations, the experimental protocols were approved by the Animal Research Ethical Committee of the University of Barcelona.

2.9.2. *In vivo and ex vivo skin tolerance*

Two squares of 5×5 cm² (left and right) were shaved with an electric razor on the back of the rabbit. One section was used as a control and the other was scraped with a lancet. 24 h later, 0.5 mL of the formulation (each separately) were applied to the shaved segments and left uncovered. After 24 h of contact between the formulations and rabbit skin, the excess was removed and the skin was macroscopic evaluated for edema and erythema according to a graduated scale of 0 to 4 in both cases. The individual primary irritancy index was determined for each rabbit based on the scale originally described by Draize (Draize et al., 1944; Zuang et al., 2005). The results allow to determine if a substance is “non-irritant”, “mildly irritant”, “moderately irritant”, or “severely irritant”. The test was performed by triplicate.

2.9.3. *Histological studies*

After macroscopic evaluation and to corroborate the results of the Draize test, histological evaluation of the tissue in contact for 24 h with the formulations was performed by optical microscopy. The samples were obtained and fixed in 4% formaldehyde, included in paraffin and stained using the eosin/hematoxylin technique (Jörundsson et al., 1999).

2.9.4. *In vivo efficacy*

The anti-inflammatory efficacy of each gel was individually evaluated using the histamine-induced wheal suppression test, in order to compare the kinetic parameters between them (Abidi et al., 2010). The procedure consists of shaving the back of the rabbit to leave an area clear of hair that allows direct visualization of the skin. Subsequently, a control site and a treatment site were determined. A total of 0.5 g of gel were applied in the treatment area, and 0.5 g of gel without HB were applied in the control area, for equality of conditions in both zones. After 1 h, with a cotton swab, any superficial excess of formulation was delicately cleaned and the test was performed. A total amount of 0.05 mL of histamine dihydrochloride solution (0.1%) were intradermal injected with an insulin syringe in both sites. 10, 20 and 30 min. after the injection, the size of the blebs generated were measured (cm²) with a caliper and compared, treatment zone versus control zone. Considering the approved protocol and the 3Rs principles (Passantino, 2008) the test was performed by triplicate.

2.10. *Skin integrity parameters (in vivo tolerance in humans)*

Based on the recommendation of the Declaration of Helsinki (General Assembly of the World Medical Association, 2014), the experimental protocol for this assay was approved by the Ethics Committee of the University of Barcelona (IRB12300003099). 20 volunteers with healthy skin, 10 men and 10 women, aged between 25 and 55 years old, gave their informed and written consent for their participation in the study. Two days before measurements and during the study, volunteers were instructed to avoid using skin care products or skin lotions on the area to be tested. On the day of the measurement, volunteers were asked to stand in the test room for at least 30 min. to stabilize at ambient conditions (25 °C and 50–60% humidity). Bio-mechanical properties measurements were made on the inside of the forearm, before and 2 h after that the formulation was uniformly applied (0.1 g/cm²). Skin temperature was measured with a Skin Thermometer® ST500 (Courage-Khazaka electronic GmbH, Cologne, Germany) as a general control parameter. The TEWL was measured with a

Tewameter® TM 300 (Courage-Khazaka electronic GmbH, Cologne, Germany) to determine the integrity of the skin barrier function and hydration of the stratum corneum was measured using a Corneometer® CM 825 (Courage-Khazaka electronic GmbH, Cologne, Germany).

2.11. *Statistical analysis*

The statistical analysis and data comparisons were achieved using two tailed *t*-test with a significance of $\alpha < 0.05$. To confirm the normality of the data and the equality of the variances, F test was accomplished. In cases where the data had abnormal distribution, Wilcoxon paired test was performed with a significance of $\alpha < 0.05$. For the data treatment GraphPad Prism® 6.01 software (GraphPad Software Inc., San Diego, CA, USA) was used and the results are presented as mean value \pm standard deviation (SD).

3. Results and discussion

3.1. *Gels characterization*

The three gels formed containing HB-NLC, presented characteristic odor due to the components and opaque white color probably due to the suspension of HB-NLC used instead of water. Cg-HB-NLC and Cb-HB-NLC showed high viscosity and low fluidity when inverting the container tube. Pl-HB-NLC was liquid at room temperature, and gelled at skin temperature (32 ± 0.5 °C). The pH, determined at 25 ± 1 °C, was maintained in the eudermic range between 5.2 and 6.5 (Jiménez et al., 2002) just after preparation and until 6 months of storage at room temperature (25 ± 2 °C) and 4 ± 2 °C.

The results of optical microscopy (Fig. 1) show that Cg-HB-NLC is a monodisperse emulsion with droplets between 4 and 5 μ m, the dark spots that are seen, have a size smaller than 1 μ m and could be HB-NLC accumulations. The gels Cb-HB-NLC and Pl-HB-NLC present a thin and homogeneous framework with particles smaller than 500 nm.

On the other hand, SEM results show for Pl-HB-NLC a moderately lax matrix generated in the aqueous HB-NLC medium by the cross-linking of the polymer fibers. These spaces of approximately 600 μ m size would allow the entry of water and the subsequent mobilization of nanoparticles (Zav \sim 200 nm) into the gel matrix, promoting their release from the formulation.

3.2. *Rheological studies and extensibility test*

The rheological results (Fig. 2) revealed that Cg-HB-NLC and Pl-HB-NLC had a pseudoplastic behavior in the ascendant and descendant stretch, having Cross equation as the best fitting model in both cases ($r^2 > 0.9998$). Thixotropic behavior was not detected in these two formulations. The viscosity at 50 s⁻¹ was 4053.11 ± 9.10 mPa·s and 325.42 ± 1.61 mPa·s, respectively. Meanwhile, Cb-HB-NLC presented a very high initial viscoelastic behavior (critical shear 8 s⁻¹) and due to thicker crisscross of the system, the viscosity could not be determined at 50 s⁻¹. However, the viscosity comparison between gels could be performed in the ascending sections for a shear rate value of 5 s⁻¹. Being respectively higher to lower viscosity Cb-HB-NLC (167.70 ± 5.03 Pa·s) > Cg-HB-NLC (22.35 ± 0.40 Pa·s) > Pl-HB-NLC (0.60 ± 0.01 Pa·s). The rigidity of the polymer network, what determines the viscosity of the formulation, induces the resistance to flow, therefore, more rigid and compact framework presents greater viscosity, as can be seen in Cb-HB-NLC (Fig. 2c), while in more fluid formulations, it assumes that crosslinking is more lax as seen in the case of Pl-HB-NLC (Fig. 2b). Before being incorporated into the gels, HB-NLC presented a Newtonian behavior and a viscosity of 1.75 ± 0.02 mPa·s regardless of the shear rate. An increase in viscosity due to the addition of gelling components could favor the stability of the HB-NLC system (Tohver et al., 2001). Repeatability was very good for Cg-HB-NLC, Pl-HB-NLC and HB-NLC suspension exhibiting variations < 2%.

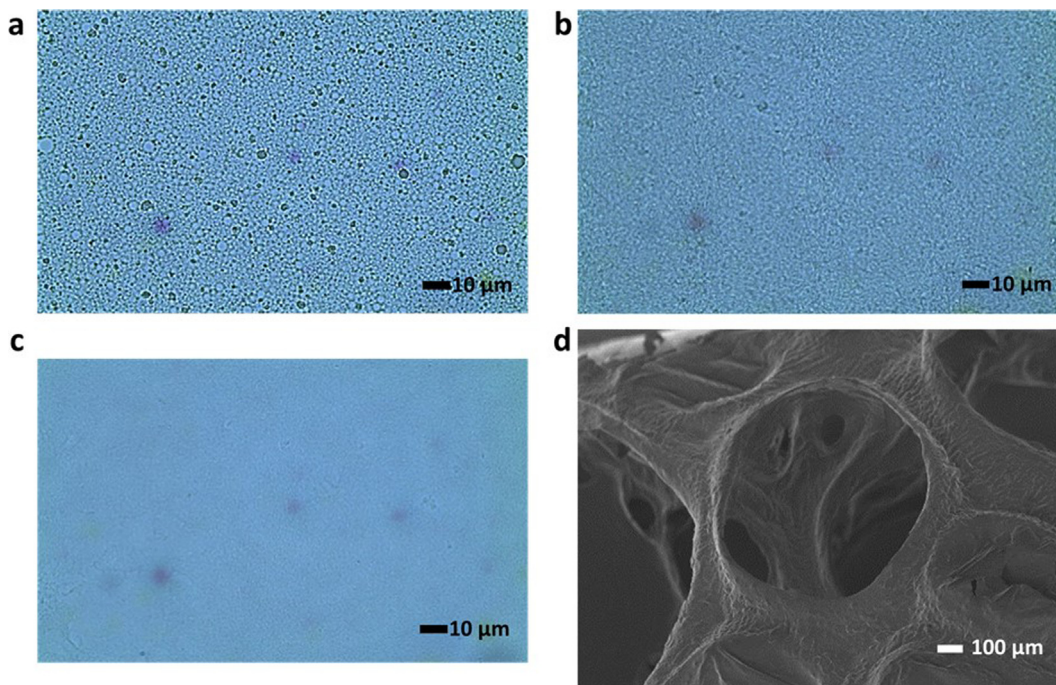


Fig. 1. Images by optical microscopy of (a) Cg-HB-NLC, (b) Cb-HB-NLC, (c) PI-HB-NLC and (d) SEM image of PI-HB-NLC.

The extensibility results performed at $25 \pm 2 \text{ }^\circ\text{C}$ are shown in Fig. 3. The linear zone of the graph where the extensibility response is proportional to the weight used, is between 20 and 100 g. It can be seen that at this temperature and 50 g compression the order of decreasing extensibility is PI-HB-NLC ($3276 \pm 15 \text{ mm}^2$) > Cg-HB-NLC

($771 \pm 14 \text{ mm}^2$) > Cb-HB-NLC ($328 \pm 17 \text{ mm}^2$). Inverse classification to that obtained with viscosity values. This is logical given that the more fluid the system, the more extensible is (Suñer-Carbó et al., 2017). In this sense, PI-HB-NLC is the most extensible and less viscous formulation, contrary to Cb-HB-NLC, where a strong elastic behavior is

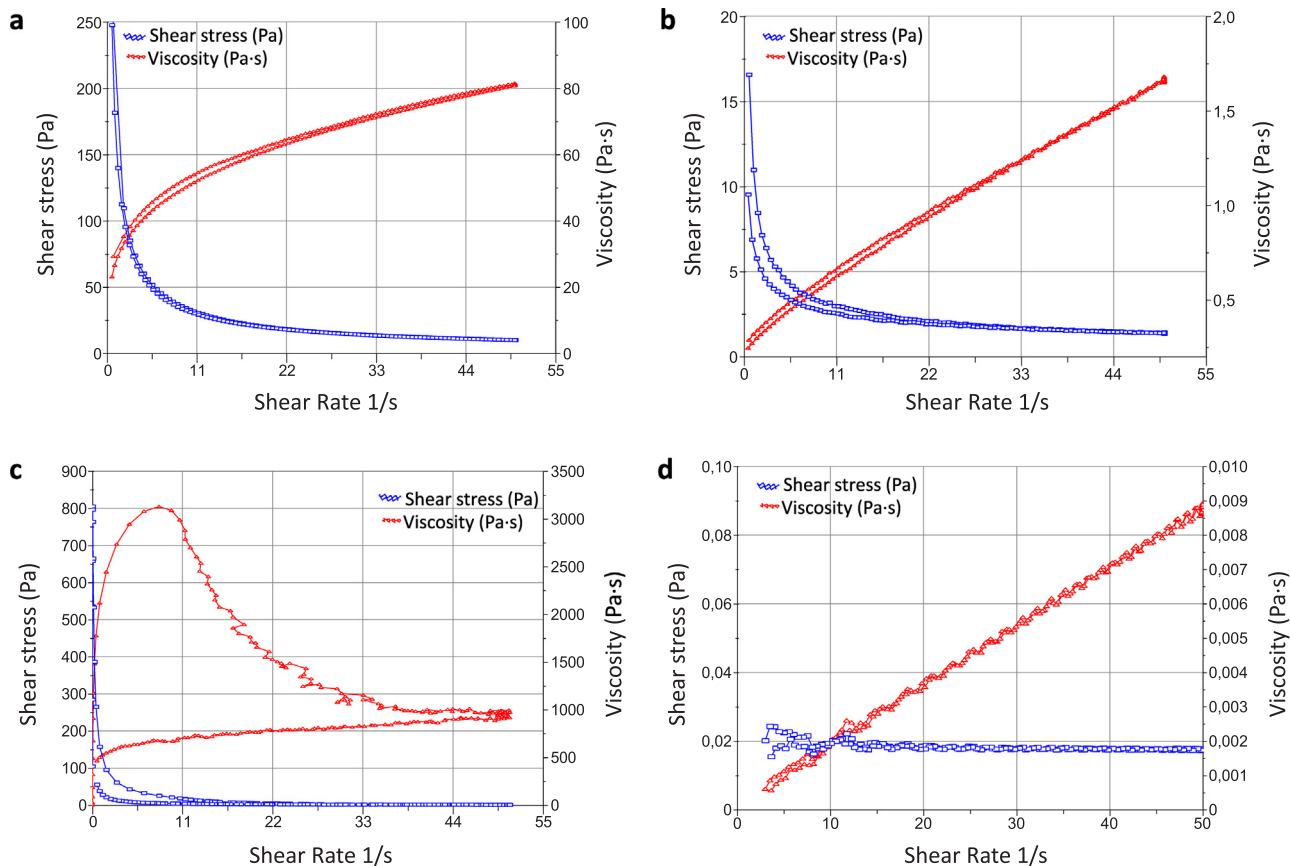


Fig. 2. Rheograms of the tested formulations measured at $25 \text{ }^\circ\text{C}$. (a) Cg-HB-NLC, (b) PI-HB-NLC, (c) Cb-HB-NLC, (d) HB-NLC suspension.

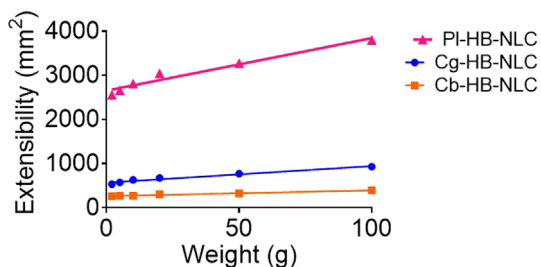


Fig. 3. Extensibility values measured at 25 °C of the Cb-HB-NLC, PI-HB-NLC and Cg-HB-NLC formulations. Results represented as mean value ± SD.

evidenced, making this gel behave more like a solid than a liquid.

3.3. Swelling, degradation test and porosity index

The swelling process of the three gels, PI-HB-NLC, Cb-HB-NLC and Cg-HB-NLC, follow a first order kinetics (Fickian kinetic) (Fig. 4) represented by the kinetic constant (k) 1.48 min^{-1} , 0.05 min^{-1} and 0.14 min^{-1} , respectively. The swelling kinetics can be affected by the pH, temperature and the ratio and concentration of the gel cross-linking (Abdul and Rajab, 2014). The results show that PI-HB-NLC is completely solubilized in 4 min reaching a $Q_{\text{max}} = 1.75\%$. Meanwhile, Cb-HB-NLC has a $Q_{\text{max}} = 7.39\%$ at 90 min and Cg-HB-NLC reaches a $Q_{\text{max}} = 1.5\%$ after 24 min. It has been described that the rate and amount of PBS captured are related to the amount of functional groups of the gelling structures, influencing the mobility of the polymer chain, thereby decreasing or increasing the SR (Samuel and Bhise, 2017). In this case, the gels have similar pH (~5), same HB-NLC water base concentration and they were treated under the same temperature which would lead us to consider that the differences are due solely to the matrix intercrossing. Cb-HB-NLC has a high cross-linking level with low flexibility (Tang et al., 2005) this would make it a more compact gel, endorsing the slower but higher PBS uptake found in comparison to PI-HB-NLC and Cg-HB-NLC which show lower level of crosslinking.

The degradation process for the studied gels showed first order kinetics (Fig. 4). This means that the weight loss depends on the concentration of polymer (gel) and therefore, that at higher concentration,

greater degradation velocity, decreasing the speed of the process over time. For PI-HB-NLC the process occurs in 80 min. with a $k = 0.04 \text{ min}^{-1}$. Whereas, for Cb-HB-NLC it occurs in 6.5 h with a $k = 0.25 \text{ h}^{-1}$ and for Cg-HB-NLC in 60 min with a $k = 0.12 \text{ min}^{-1}$. The differences between the gels could be due to the level of cross-linking of the polymer, for Cb-HB-NLC, the polymer has a high level of cross-linking with low flexibility (Tang et al., 2005) which could influence reducing the speed of the process. While for laxer cross-linking formulations such as PI-HB-NLC, the process would be favored (Mallandrich et al., 2017).

The results of P in decreasing order were $5.82 \pm 1.04\%$ for PI-HB-NLC > $0.89 \pm 0.12\%$ for Cg-HB-NLC and $0.48 \pm 0.07\%$ for Cb-HB-NLC. A decreased P could occur due to an increase in the concentration of the cross-linking agent, increasing the association between the monomer and the polymer (Bukhari et al., 2015). On the other hand, gels with a small pore size have a strong viscous coupling between the formed network and the solvent, suppressing the movement of the polymer network in relation to the solvent (de Cagny et al., 2016). These P results are in agreement with the viscosity values where Cb-HB-NLC has lower P and high viscosity, contrary to PI-HB-NLC, where a higher P correlates with a lower viscosity.

3.4. Stability test

The physical stability of the samples stored at 4 and 25 °C revealed that the gels are highly stable for more than 6 months at both temperatures (Fig. 5). However in comparison, Cg-HB-NLC showed slightly changes at 25 °C (Fig. 5d), probably because its composition is more complex than PI-HB-NLC and Cb-HB-NLC. The temperature would alter the interaction between the lipid and polymer components, promoting cross-linking alteration and therefore promoting the instability of the sample (Limón et al., 2015; Ji et al., 2015). Considering the obtained results, even if both storage temperatures are adequate, the temperature at which the formulations remain more stable is at 4 °C, which is consistent with the temperature storage for HB-NLC suspension. Before incorporation into the gels, HB-NLC proved to be stable by itself for one month (Carvajal-Vidal et al., 2019). So, the incorporation of the HB-NLC into the gel matrix, improves their storage stability 6 times. These results are in accordance and could be explained by viscosity changes. A

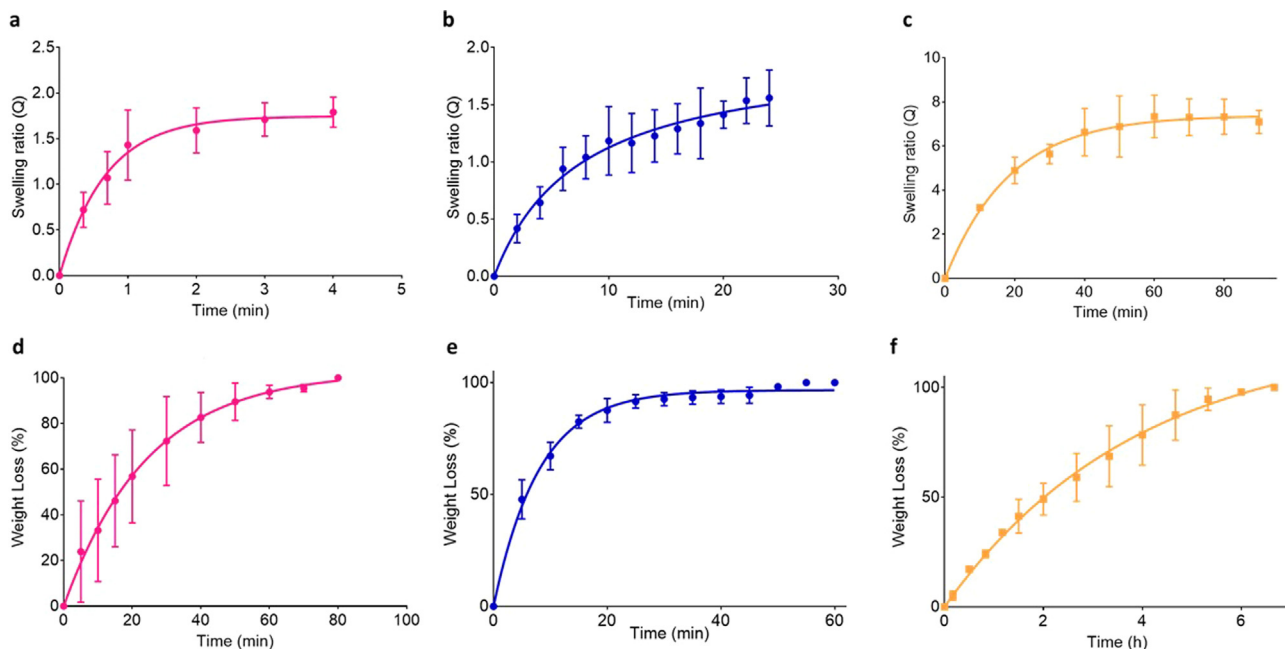


Fig. 4. Swelling kinetics of (a) PI-HB-NLC, (b) Cg-HB-NLC, (c) Cb-HB-NLC and WL% of (d) PI-HB-NLC, (e) Cg-HB-NLC, (f) Cb-HB-NLC. Results represented as mean ± SD.

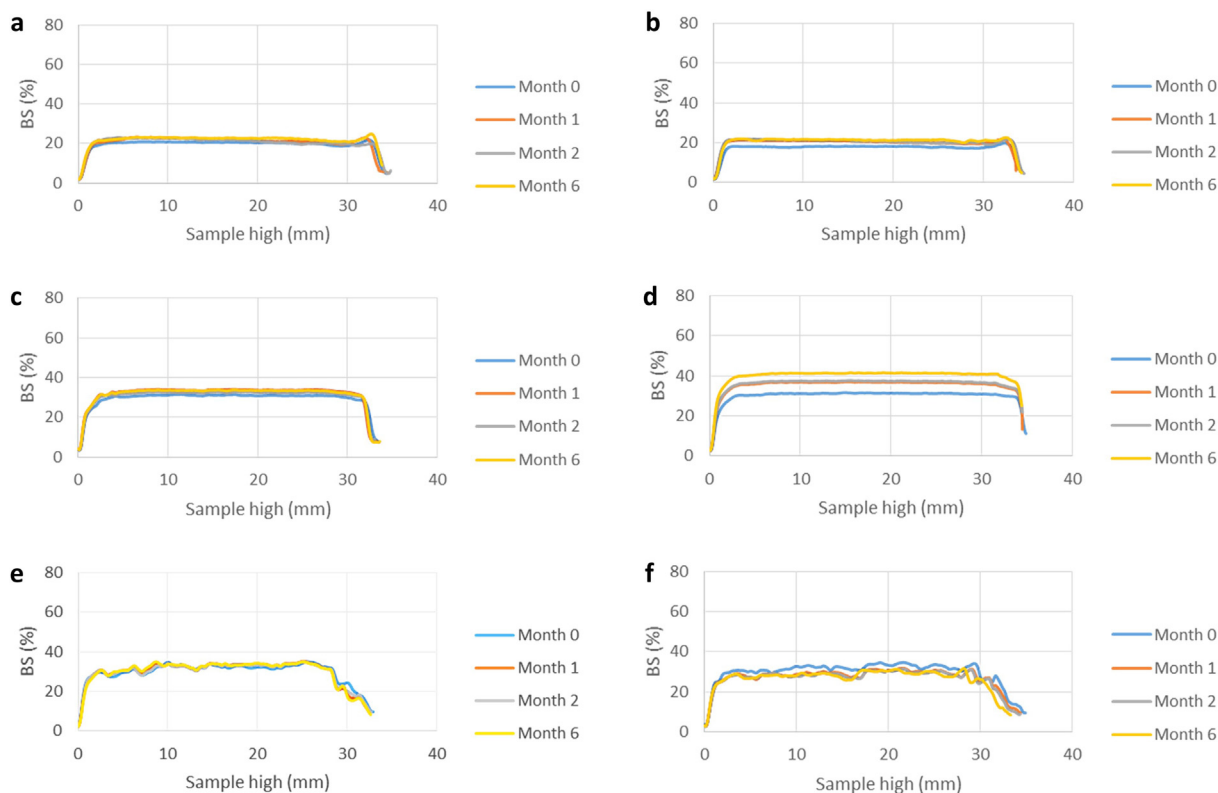


Fig. 5. Backscattering gels profiles of PI-HB-NLC at 4 °C (a) and 25 °C (b), Cg-HB-NLC at 4 °C (c) and 25 °C (d), Cb-HB-NLC at 4 °C (e) and 25 °C (f).

more viscous matrix would decrease the free movement of the particles, and their aggregation or sedimentation could be delayed or even avoided compared to the original aqueous system.

3.5. Microbiological assay

All evaluated products showed the same behavior at microbiological level, those stored at room temperature and at 4 °C. Regarding the total mesophilic, fungal and yeast count, we can conclude that the bacterial load is less than 10 cfu/g in all samples. Seeding in the corresponding selective media from the enrichments in TSB broth, allowed to verify the absence of pathogenic microorganisms such as *Staphylococcus aureus*, *Pseudomonas aeruginosa*, *Escherichia coli* and *Candida albicans*. The gels were formulated without a preservative medium, therefore the absence of microbiological growth, could mean that the amount of free water in the formulations is not enough to promote the proliferation of microorganisms or that the components of the nanoparticles (despite being lipid) do not favor the microbiological multiplication.

3.6. Biopharmaceutical behavior

3.6.1. In vitro release

The *in vitro* release profile, determined by Franz cells are shown in Fig. 6a. As can be seen, during the first h. there is a rapid release of HB, reaching a 62.5% from Cb-HB-NLC at 100 h, which continues increasing until it becomes sustained without achieving the plateau during the study period. The same happens with PI-HB-NLC, the plateau is not evident, but it can be seen that the release process is much slower, reaching only a 49.8% of HB released in 300 h. This behavior could be due to the lipid characteristics of the drug, because its solubility in the polymer matrix is disadvantaged in contrast to NLC matrix, thus delaying the diffusion of HB from the NLC (Roseman, 1972). In comparison, Cg-HB-NLC seems to release a maximum of 65.3% of the total formulation content at 220 h. PI-HB-NLC and Cg-HB-NLC follows a first order kinetics, with an initially rapid and subsequently sustained

release over time, characteristic of SLN (Venkateswarlu and Manjunath, 2004). Cb-HB-NLC kinetics correspond to a hyperbolic model, although its mathematical adjustment value is very similar also to first order. The release of HB follows the same kinetics from gel, as when released from the NLC, but slower (Carvajal-Vidal et al., 2019) because in this case, the drug follows a series of events, which includes its release from the NLC and then spreading between the gel matrix, thus slowing the release rate from the total formulation (Joshi and Patravale, 2008). Both, rapid release and sustained release are beneficial for dermal treatment, the first one allows to exert an initial effect while sustained release allows to provide the drug for a prolonged period of time.

3.6.2. Ex vivo permeation

The permeation study was performed on human skin for 36 h, during this period, the stratum corneum integrity is guaranteed, and so, its ability to act as a membrane is maintained intact (Mallandrich et al., 2017). Fig. 6b shows at 36 h a penetration of 0.06, 0.61 and 0.97 µg for PI-HB-NLC, Cg-HB-NLC and Cb-HB-NLC, respectively. Comparatively it is observed that at 24 h. Cb-HB-NLC permeates 1.6 times more than Cg-HB-NLC and 16 times more than PI-HB-NLC, with an equivalent initial sample concentration, this means that these values are in agreement with the drug's release profiles, in the face of a faster release, faster skin penetration occurs in every measured time, what could indicate that the permeation is mainly determined by HB diffusion from the gels. The results indicate that the drug permeation from the gels is much slower compared to the free drug and even the drug in an HB-NLC suspension (Carvajal-Vidal et al., 2019), which might suggest that the drug stays longer on the skin surface before going into systemic circulation.

3.7. In vivo and ex vivo tolerance

The results of the Draize's test show that there was no evidence of damage, no edema or erythema produced by direct contact with the formulations, classifying them as non-irritants.

In the histological study (Fig. 7) can be observed that the skin

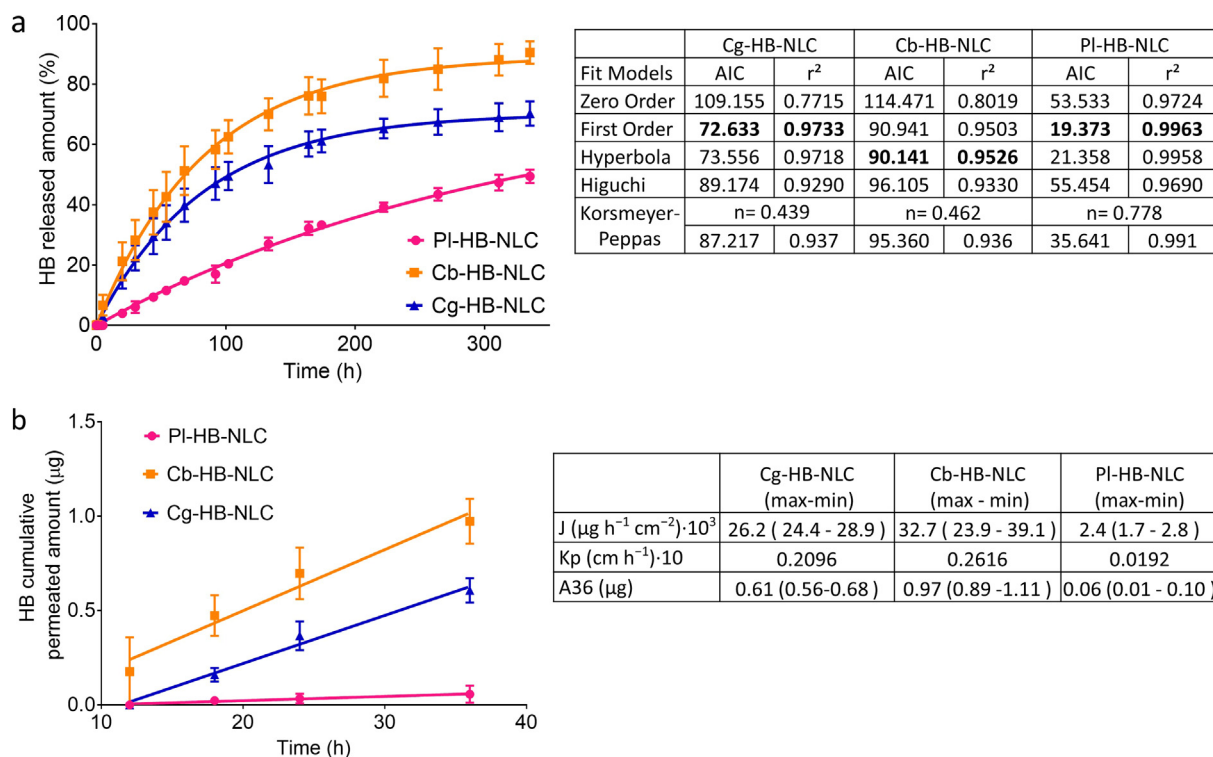


Fig. 6. Biopharmaceutical behavior. (a) *In vitro* release profiles of HB from different gels (adjusted to kinetics), (b) *Ex vivo* human skin permeation profile of HB from different gels and permeation parameters. Results represented as mean ± SD.

structures remain organized after application of the gels, there is no significant damage at the histological level between the areas in contact with the formulations in comparison with the control (Fig. 7a). This confirms that the formulations do not incite any disruption in the skin

layers after 24 h direct contact, verifying that the mixtures of components used to make the formulations have no negative effect and they are safe for their intended use.

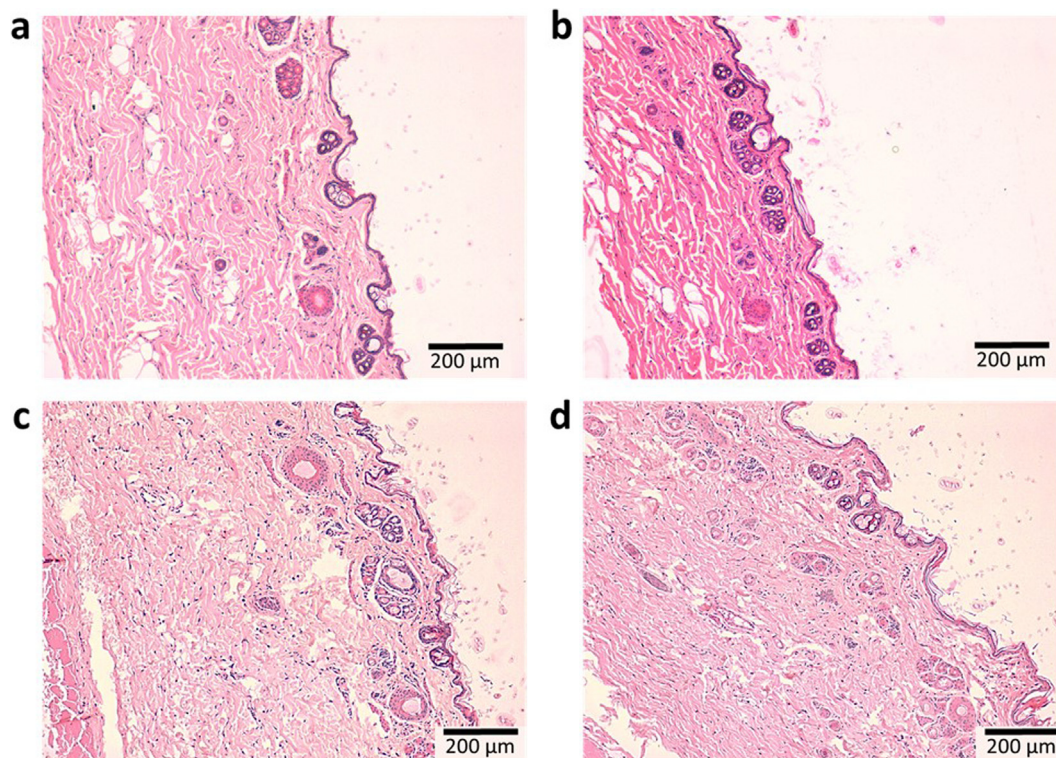


Fig. 7. Histological analysis of rabbits back, blank and in contact areas. (a) No contact skin. Skin in contact with formulation for 24 h (b) PI-HB-NLC, (c) Cb-HB-NLC, (d) Cg-HB-NLC.

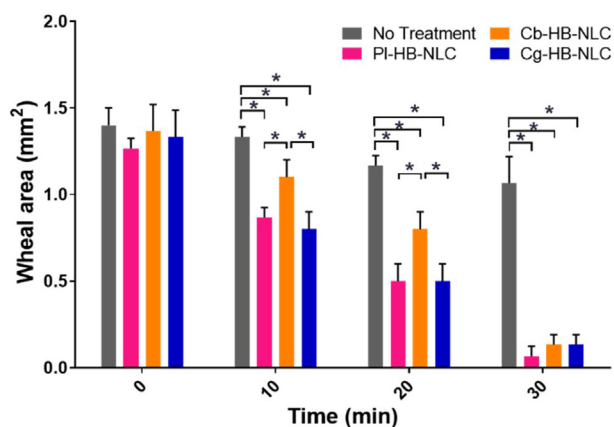


Fig. 8. Efficacy results. *In vivo* histamine-induced wheal suppression test results represented as mean ± SD. Statistically significant differences are represented with * ($p < 0.005$).

3.8. Anti-inflammatory efficacy

In Fig. 8 it can be seen that from the 10 min of the application of the gels, there is an anti-inflammatory effect in comparison with the control. The bleb formation is smaller in every case with a reduction of 35.0%, 17.5% and 40.0% for PI-HB-NLC, Cb-HB-NLC and Cg-HB-NLC, respectively. At 30 min, it can be seen that the effect does not present statistically significant differences between gels, but the blebs are 87.5% reduced in comparison with the control. These results demonstrate the anti-inflammatory efficacy of the formulations. PI-HB-NLC shows a constant and evident decrease of the inflammation, probably due to the polymeric matrix, that allows the movement of the HB-NLC out from the formulation, in comparison with Cb-HB-NLC, which, being more viscous and with a thicker matrix, limits the output of HB-NLC, therefore, causing a slower release and a slower anti-inflammatory immediate effect. Considering the permeated parameters obtained in *ex vivo* results, we could infer that presenting lower values in

permeation parameters, would increase the drug time within the skin. A slower drug penetration through the skin would probably be in accordance with a higher drug retention in the skin, which would lead to reaching the drug needed amount to activate the local corticosteroid receptors earlier, which would trigger faster initial local effect.

3.9. Skin integrity parameters (Tolerance in human)

TEWL values indicate no statistically significant differences between the control and PI-HB-NLC (tendency to decrease of 7.2%), but, the formulations Cb-HB-NLC and Cg-HB-NLC showed a decrease in values ($p < 0.05$) of 9.2% and 21.8% respectively, after 2 h of use (Fig. 9a, b, c). The formulations are well tolerated and it can be considered that they have protective action. Ever since TEWL measures the trans-epidermal water lost, this parameter can be considered as a measure of the integrity of the skin, where a maintenance or a decrease in value is indicative that the tested formulations are suitable for use on skin, since it maintains its barrier properties. On the contrary, an increase in TEWL values would indicate that the evaporation of water through the skin has increased and therefore, the stratum corneum is altered, decreasing its protective barrier function (Akdeniz et al., 2018).

The hydration of the stratum corneum was determined measuring the changes in the dielectric capacity of the skin by corneometry. Fig. 9(d, e, f) shows a statistically significant ($p < 0.05$) increase of 55.7% hydration 2 h after application of Cg-HB-NLC, while Cb-HB-NLC did not show a significant variations with respect to the initial value, but had an increasing tendency of 2.7%. This could be attributed to a possible immediate moisturizing effect of the gels (Bogdan et al., 2017). The hydration decrease presented by PI-HB-NLC (39.2%) could be attributed to a superficial film formed by the gel, a film with an opaque, dry and rough appearance, visible and evident to the touch that probably acted as an artifact, preventing the correct interaction between the measurement probe and the skin, providing highly diminished hydration values. After application of the formulations, the biomechanical properties indicate that they would have a protective and moisturizing effect by maintaining/decreasing TEWL values and increasing

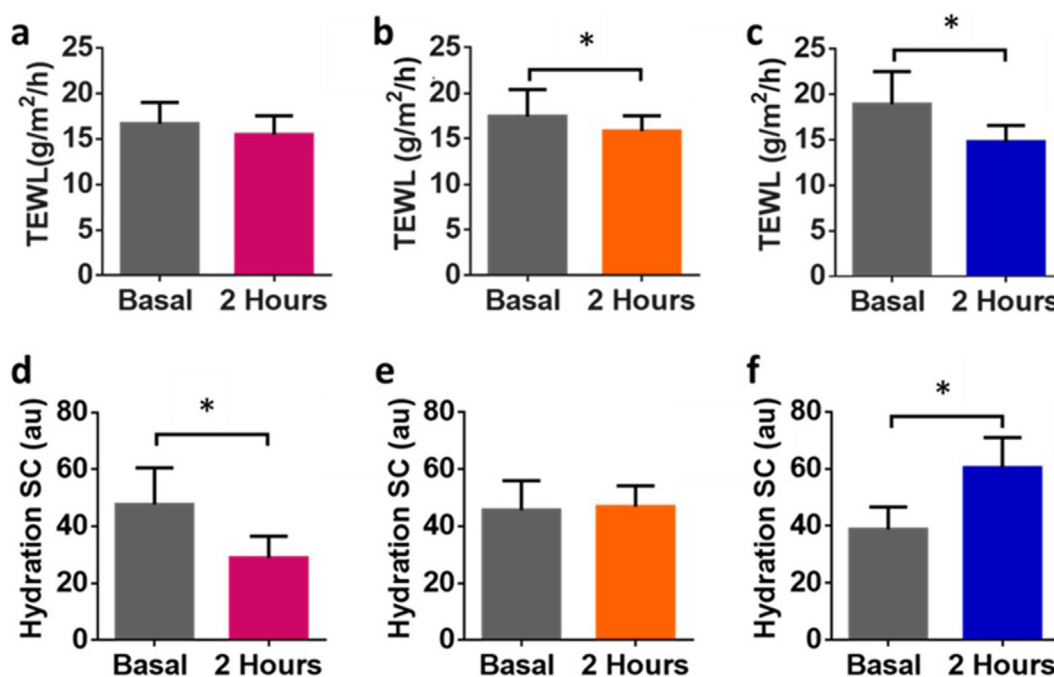


Fig. 9. Skin biomechanical properties. Measures made on 20 healthy volunteers. TEWL determinations: PI-HB-NLC (a), Cb-HB-NLC (b) and Cg-HB-NLC (c). SC hydration determinations: PI-HB-NLC (d), Cb-HB-NLC (e) and Cg-HB-NLC (f). Due to the great variability of the skin for these type of measurement, the data does not have a normal distribution. Non-parametric Wilcoxon matched-pairs signed rank was selected as the best statistical test for biomechanical properties analysis. Results represented as mean ± SD.

hydration, respectively, especially for Cg-HB-NLC. A wide variety of skin diseases present dryness and irritation and as a result, it produces itching and scaling of the stratum corneum, getting worse basal disease. The results show that the formulations developed would be a suitable vehicle for HB-NLC, but they could also reduce the physical discomfort associated with the disease, helping to better control the symptoms.

4. Conclusion

The concentration and characteristics of the polymer used in a gel dosage form loaded nanoparticles for topical administration constitutes a key factor to determine if the drug will have immediate or sustained effect, allowing to modulate its release, while acting on the properties of the skin. The results of this research indicate that the PI-HB-NLC, Cb-HB-NLC and Cg-HB-NLC gels have anti-inflammatory pharmacological effect and are suitable for their use on skin for prolonged periods of time, making possible the administration of the drug in different vehicles that offers the opportunity to select the most appropriate one, according to the skin conditions of a specific patient, not only to treat the underlying disease, but also to reduce the discomfort of the associated symptomatology.

CRedit authorship contribution statement

Paulina Carvajal-Vidal: Conceptualization, Methodology, Formal analysis, Investigation, Writing - original draft, Visualization. **Roberto González-Pizarro:** Validation, Formal analysis, Investigation. **Carolina Araya:** Investigation. **Marta Espina:** Formal analysis, Writing - review & editing. **Lyda Halbaut:** Methodology, Validation. **Immaculada Gómez de Aranda:** Investigation. **M. Luisa García:** Conceptualization, Supervision, Writing - review & editing, Project administration. **Ana Calpena:** Conceptualization, Methodology, Formal analysis, Supervision.

Declaration of Competing Interest

The authors declare that they have no known competing financial interests or personal relationships that could have appeared to influence the work reported in this paper.

Acknowledgements

Thanks to “Comisión Nacional de Investigación Científica y Tecnológica” (CONICYT) Chile, [2014-72150377 for a PhD grant (P.A.C-V)].

References

Abdul, B.I., Rajab, N.A., 2014. Preparation and in-vitro evaluation of mucoadhesive clotrimazole vaginal hydrogel. *Iraqi Journal of Pharmaceutical Sciences* (P-ISSN: 1683 - 3597, E-ISSN : 2521 - 3512), 23(1), 19-25.

Abidi, A., Ahmad, F., Singh, S.K., Kumar, A., 2010. Study of reservoir effect of clobetasol propionate cream in an experimental animal model using histamine-induced wheal suppression test. *Indian J. Dermatol.* 55 (4), 329–333. <https://doi.org/10.4103/0019-5154.74531>.

Akdeniz, M., Gabriel, S., Lichterfeld-Kottner, A., Blume-Peytavi, U., Kottner, J., 2018. Transepidermal water loss in healthy adults: a systematic review and meta-analysis update. *Br. J. Dermatol.* 179 (5), 1049–1055. <https://doi.org/10.1111/bjd.17025>.

Al-Dabagh, A., Al-Dabagh, R., Davis, S.A., Taheri, A., Lin, H.-C., Balkrishnan, R., Feldman, S.R., 2014. Systemic corticosteroids are frequently prescribed for psoriasis. *J. Cutaneous Med. Surg.* 18 (3), 195–199. <https://doi.org/10.2310/7750.2013.13126>.

Barshack, I., Kopolovic, J., Chowers, Y., Gileadi, O., Vainshtein, A., Zik, O., Behar, V., 2004. A novel method for «Wet» SEM. *Ultrastruct. Pathol.* 28 (1), 29–31.

Berrozo, J.D., Lanao, J.M., Delfina, J.M.P., 2008. *Biofarmacia y farmacocinética*. Madrid, España. Ed. Síntesis.

Bikkad, M.L., Nathani, A.H., Mandlik, S.K., Shrotriya, S.N., Rampise, N.S., 2014. Halobetasol propionate-loaded solid lipid nanoparticles (SLN) for skin targeting by topical delivery. *J. Liposome Res.* 24 (2), 113–123. <https://doi.org/10.3109/08982104.2013.843192>.

Bogdan, C., Iurian, S., Tomuta, I., Moldovan, M., 2017. Improvement of skin condition in *striae distensae*: development, characterization and clinical efficacy of a cosmetic

product containing *Punica granatum* seed oil and *Croton lechleri* resin extract. *Drug Des., Dev. Therapy* 11, 521–531. <https://doi.org/10.2147/DDDT.S128470>.

Boguniewicz, M., Leung, D.Y.M., 2011. Atopic dermatitis: a disease of altered skin barrier and immune dysregulation. *Immunol. Rev.* 242 (1), 233–246. <https://doi.org/10.1111/j.1600-065X.2011.01027.x>.

Brugués, A.P., Naveros, B.C., Calpena Campmany, A.C., Pastor, P.H., Saladrigas, R.F., Lizandra, C.R., 2015. Developing cutaneous applications of paromomycin entrapped in stimuli-sensitive block copolymer nanogel dispersions. *Nanomedicine (London)* 10 (2), 227–240. <https://doi.org/10.2217/nmm.14.102>.

Bukhari, S.M.H., Khan, S., Rehanullah, M., Ranjha, N.M., 2015. Synthesis and characterization of chemically cross-linked acrylic acid/gelatin hydrogels: effect of pH and composition on swelling and drug release. *Int. J. Polymer Sci. (Special issue)*. <https://doi.org/10.1155/2015/187961>.

Campaña-Seoane, M., Peleteiro, A., Laguna, R., Otero-Espinar, F.J., 2014. Bioadhesive emulsions for control release of progesterone resistant to vaginal fluids clearance. *Int. J. Pharm.* 477 (1), 495–505. <https://doi.org/10.1016/j.ijpharm.2014.10.066>.

Carvajal-Vidal, P., Mallandrich, M., García, M.L., Calpena, A.C., 2017. Effect of different skin penetration promoters in halobetasol propionate permeation and retention in human skin. *Int. J. Mol. Sci.* 18 (11), 2475. <https://doi.org/10.3390/ijms18112475>.

Carvajal-Vidal, P., Fábrega, M.-J., Espina, M., Calpena, A.C., García, M.L., 2019. Development of Halobetasol-loaded nanostructured lipid carrier for dermal administration: optimization, physicochemical and biopharmaceutical behavior, and therapeutic efficacy. *Nanomed. Nanotechnol. Biol. Med.* 20, 102026. <https://doi.org/10.1016/j.nano.2019.102026>.

Costa, P., Sousa Lobo, J.M., 2001. Modeling and comparison of dissolution profiles. *Eur. J. Pharm. Sci.* 13 (2), 123–133. [https://doi.org/10.1016/S0928-0987\(01\)00095-1](https://doi.org/10.1016/S0928-0987(01)00095-1).

Coureau, B., Bussièrès, J.-F., Tremblay, S., 2008. Cushing's syndrome induced by misuse of moderate- to high-potency topical corticosteroids. *Ann. Pharmacother.* 42 (12), 1903–1907. <https://doi.org/10.1345/aph.1L067>.

de Cagny, H.C.G., Vos, B.E., Vahabi, M., Kurniawan, N.A., Doi, M., Koenderink, G.H., Bonn, D., 2016. Porosity governs normal stresses in polymer gels. *Phys. Rev. Lett.* 117 (21), 217802. <https://doi.org/10.1103/PhysRevLett.117.217802>.

Dhar, S., Seth, J., Parikh, D., 2014. Systemic side-effects of topical corticosteroids. *Indian J. Dermatol.* 59 (5), 460–464. <https://doi.org/10.4103/0019-5154.139874>.

Draize, J.H., Woodard, G., Calvery, H.O., 1944. Methods for the study of irritation and toxicity of substances applied topically to the skin and mucous membranes. *J. Pharmacol. Exp. Ther.* 82 (3), 377–390.

Eyerich, K., Novak, N., 2013. Immunology of atopic eczema: overcoming the Th1/Th2 paradigm. *Allergy* 68 (8), 974–982. <https://doi.org/10.1111/all.12184>.

General Assembly of the World Medical Association, 2014. World medical association declaration of Helsinki: ethical principles for medical research involving human subjects. *The Journal of the American College of Dentists*, 81(3), 14–18.

Gonzalez-Pizarro, R., Carvajal-Vidal, P., Halbaut Bellowa, L., Calpena, A. C., Espina, M., & García, M. L., 2019. In-situ forming gels containing fluorometholone-loaded polymeric nanoparticles for ocular inflammatory conditions. *Colloids and Surfaces B: Bio interfaces*, 175, 365-374. DOI:10.1016/j.colsurfb.2018.11.065.

Herz, G., Blum, G., Yawalkar, S., 1991. Halobetasol propionate cream by day and Halobetasol propionate ointment at night for the treatment of pediatric patients with chronic, localized plaque psoriasis and atopic dermatitis. *J. Am. Acad. Dermatol.* 25, 1166–1169. [https://doi.org/10.1016/0190-9622\(91\)70319-W](https://doi.org/10.1016/0190-9622(91)70319-W).

Jensen, L.B., Magnusson, E., Gunnarsson, L., Vermehren, C., Nielsen, H.M., Petersson, K., 2010. Corticosteroid solubility and lipid polarity control release from solid lipid nanoparticles. *Int. J. Pharm.* 390 (1), 53–60. <https://doi.org/10.1016/j.ijpharm.2009.10.022>.

Ji, J., Zhang, J., Chen, J., Wang, Y., Dong, N., Hu, C., Wu, C., 2015. Preparation and stabilization of emulsions stabilized by mixed sodium caseinate and soy protein isolate. *Food Hydrocolloids* 51, 156–216. <https://doi.org/10.1016/j.foodhyd.2015.05.013>.

Jiménez, M.M., Fresno, M.C., Sellés, E., 2002. Pharmacotechnical characterization and effectiveness testing of a proposed emulsion for the treatment of dry skin. *Boll. Chim. Farm.* 141 (5), 333–342.

Jörundsson, E., Lumsden, J.H., Jacobs, R.M., 1999. Rapid staining techniques in cytopathology: a review and comparison of modified protocols for hematoxylin and eosin, Papanicolaou and Romanowsky stains. *Veterinary Clin. Pathol.* 28 (3), 100–108. <https://doi.org/10.1111/j.1939-165X.1999.tb01057.x>.

Joshi, M., Patravale, V., 2008. Nanostructured lipid carrier (NLC) based gel of celecoxib. *Int. J. Pharm.* 346 (1), 124–132. <https://doi.org/10.1016/j.ijpharm.2007.05.060>.

Lee, J.H., Bucknall, D.G., 2008. Swelling behavior and network structure of hydrogels synthesized using controlled UV-initiated free radical polymerization. *J. Polym. Sci., Part B: Polym. Phys.* 46 (14), 1450–1462. <https://doi.org/10.1002/polb.21481>.

Limón, D., Amirthalingam, E., Rodrigues, M., Halbaut, L., Andrade, B., Garduño-Ramírez, M.L., Calpena, A.C., 2015. Novel nanostructured supramolecular hydrogels for the topical delivery of anionic drugs. *Eur. J. Pharm. Biopharm.* 96, 421–436. <https://doi.org/10.1016/j.ejpb.2015.09.007>.

Lowe, N., Feldman, S.R., Sherer, D., Weiss, J., Shavin, J.S., Lin, Y.L., Soto, P., 2005. Clobetasol propionate lotion, an efficient and safe alternative to clobetasol propionate emollient cream in subjects with moderate to severe plaque-type psoriasis. *J. Dermatol. Treatment* 16 (3), 158–164. <https://doi.org/10.1080/09546630510041060>.

Mallandrich, M., Fernández-Campos, F., Clares, B., Halbaut, L., Alonso, C., Coderch, L., Calpena, A.C., 2017. Developing transdermal applications of ketorolac tromethamine entrapped in stimuli sensitive block copolymer hydrogels. *Pharm. Res.* 34 (8), 1728–1740. <https://doi.org/10.1007/s11095-017-2181-8>.

Mancuso, G., Balducci, A., Casadio, C., Farina, P., Staffa, M., Valenti, L., Milani, M., 2003. Efficacy of betamethasone valerate foam formulation in comparison with betamethasone dipropionate lotion in the treatment of mild-to-moderate alopecia areata:

- a multicenter, prospective, randomized, controlled, investigator-blinded trial. *Int. J. Dermatol.* 42 (7), 572–575. <https://doi.org/10.1046/j.1365-4362.2003.01862.x>.
- Müller, Rainer H., Mäder, K., Gohla, S., 2000. Solid lipid nanoparticles (SLN) for controlled drug delivery – a review of the state of the art. *Eur. J. Pharm. Biopharm.* 50 (1), 161–177. [https://doi.org/10.1016/S0939-6411\(00\)00087-4](https://doi.org/10.1016/S0939-6411(00)00087-4).
- Müller, R.H., Petersen, R.D., Hommoss, A., Pardeike, J., 2007. Nanostructured lipid carriers (NLC) in cosmetic dermal products. *Adv. Drug Deliv. Rev.* 59 (6), 522–530. <https://doi.org/10.1016/j.addr.2007.04.012>.
- Neupane, Y.R., Srivastava, M., Ahmad, N., Kumar, N., Bhatnagar, A., Kohli, K., 2014. Lipid based nano-carrier system for the potential oral delivery of decitabine: formulation design, characterization, *ex vivo*, and *in vivo* assessment. *Int. J. Pharm.* 477 (1), 601–612. <https://doi.org/10.1016/j.ijpharm.2014.11.001>.
- Organization for Economic Co-Operation and Development (OECD), Guidelines for the Testing of chemicals. Section 4 test no. 404: acute dermal irritation/corrosion. Available online: <https://www.oecd.org/env/test-no-404-acute-dermal-irritation-corrosion-9789264242678-en.htm> (accessed 19.08.2019).
- Pasparakis, M., Haase, I., Nestle, F.O., 2014. Mechanisms regulating skin immunity and inflammation. *Nat. Rev. Immunol.* 14 (5), 289–301. <https://doi.org/10.1038/nri3646>.
- Passantino, A., 2008. Application of the 3Rs principles for animals used for experiments at the beginning of the 21st century. *Ann. Rev. Biomed. Sci.* 10, 27–32.
- Ramamoorthy, S., Cidlowski, J.A., 2016. Corticosteroids: mechanisms of action in health and disease. *Rheumatic Dis. Clin.* 42 (1), 15–31. <https://doi.org/10.1016/j.rdc.2015.08.002>.
- Ramos, G.Y., García, M.L., Espina, M., Parra, A., Calpena, A.C., 2016. Influence of freeze-drying and γ -irradiation in preclinical studies of flurbiprofen polymeric nanoparticles for ocular delivery using d-(+)-trehalose and polyethylene glycol. *Int. J. Nanomed.* 11, 4093–4106. <https://doi.org/10.2147/IJN.S105606>, [10.2147/IJN.S105606](https://doi.org/10.2147/IJN.S105606).
- Ratajczak, M., Kubicka, M.M., Kamińska, D., Sawicka, P., Długaszewska, J., 2015. Microbiological quality of non-sterile pharmaceutical products. *Saudi Pharm. J.* 23 (3), 303–307. <https://doi.org/10.1016/j.jpsps.2014.11.015>.
- Roseman, T.J., 1972. Release of steroids from a silicone polymer. *J. Pharm. Sci.* 61 (1), 46–50. <https://doi.org/10.1002/jps.2600610106>.
- Samuel, A.J., Bhise, K.S., 2017. Hydrogels: n intelligent carrier for targeted drug delivery. *Asian J. Pharm. Res. Dev.* 1–9.
- Suñer-Carbó, J., Boix-Montañés, A., Halbaut-Bellowa, L., Velázquez-Carralero, N., Zamarbide-Ledesma, J., Bozal-de-Febrer, N., Calpena-Campmany, A.C., 2017. Skin permeation of econazole nitrate formulated in an enhanced hydrophilic multiple emulsion. *Mycoses* 60 (3), 166–177. <https://doi.org/10.1111/myc.12575>.
- Tang, C., Yin, C., Pei, Y., Zhang, M., Wu, L., 2005. New super porous hydrogels composites based on aqueous Carbopol® solution (SPHCs): synthesis, characterization and *in vitro* bioadhesive force studies. *Eur. Polym. J.* 41 (3), 557–562. <https://doi.org/10.1016/j.eurpolymj.2004.10.017>.
- Tohver, V., Smay, J.E., Braem, A., Braun, P.V., Lewis, J.A., 2001. Nanoparticle halos: a new colloid stabilization mechanism. *Proc. Natl. Acad. Sci.* 98 (16), 8950–8954. <https://doi.org/10.1073/pnas.151063098>.
- Venkateswarlu, V., Manjunath, K., 2004. Preparation, characterization and *in vitro* release kinetics of clozapine solid lipid nanoparticles. *J. Control. Release* 95 (3), 627–638. <https://doi.org/10.1016/j.jconrel.2004.01.005>.
- Zhao, Y., Su, H., Fang, L., Tan, T., 2005. Superabsorbent hydrogels from poly (aspartic acid) with salt-, temperature- and pH-responsiveness properties. *Polymer* 46 (14), 5368–5376. <https://doi.org/10.1016/j.polymer.2005.04.015>.
- Zuang, V., Alonso, M.A., Botham, P.A., Eskes, C., Fentem, J., Liebsch, M., van de Sandt, J.J.M., 2005. 3.2. Skin irritation and corrosion. *Altern. Lab. Anim.* 33, 35–46. <https://doi.org/10.1177/026119290503301s08>.